Structure factors for tunneling ionization rates of molecules

Lars Bojer Madsen,[1] Frank Jensen,[2] Oleg I. Tolstikhin,[3,4] and Toru Morishita[5]

[1]*Lundbeck Foundation Theoretical Center for Quantum System Research, Department of Physics and Astronomy, Aarhus University, 8000 Aarhus C, Denmark*

[2]*Department of Chemistry, Aarhus University, 8000 Aarhus C, Denmark*

[3]*National Research Center "Kurchatov Institute," Kurchatov Square 1, Moscow 123182, Russia*

[4]*Moscow Institute of Physics and Technology, Dolgoprudny 141700, Russia*

[5]*Department of Engineering Science, The University of Electro-Communications, 1-5-1 Chofu-ga-oka, Chofu-shi, Tokyo 182-8585, Japan*

(Received 23 November 2012; published 7 January 2013)

Within the weak-field asymptotic theory, the dependence of the tunneling ionization rate of a molecule in a static electric field on its orientation with respect to the field is determined by the structure factor for the highest occupied molecular orbital (HOMO). An accurate determination of this factor, and hence the ionization rate, requires accurate values of the HOMO in the asymptotic region. Techniques for calculating the structure factors for molecules in the Hartree-Fock approximation are discussed. For diatomics, grid-based numerical Hartree-Fock calculations which reproduce the correct asymptotic tail of the HOMO are possible. However, for larger molecules, to solve the Hartree-Fock equations one should resort to basis-based approaches with too rapidly decaying Gaussian basis functions. A systematic study of the possibility to reproduce the asymptotic tail of the HOMO in calculations with Gaussian basis sets is presented. We find that polarization-consistent basis sets with quadruple or pentuple-zeta quality greatly improve the tail of the HOMO, but only when used with variationally optimized exponents. This methodology is validated by considering the CO molecule for which reliable grid-based calculations can be performed. The optimized Gaussian basis sets are used to calculate the structure factors for the triatomic molecules CO_2 and OCS. The results are compared with available experimental and theoretical results.

DOI: 10.1103/PhysRevA.87.013406 PACS number(s): 32.80.Rm, 33.80.Rv, 42.50.Hz

I. INTRODUCTION

Tunneling ionization of atoms and molecules by intense low-frequency laser pulses launches a variety of processes of current interest in strong-field physics and attoscience [1,2]. Accurate tunneling ionization rates are naturally required for the analysis of experimentally observable photoelectron and harmonic generation spectra and retrieving the target structure information (see, e.g., Refs. [3–9] and references therein). This paper continues our previous work on the weak-field asymptotic theory (WFAT) of tunneling ionization of molecules [10,11], focusing on techniques for calculating the molecular structure factors.

The theoretical description of ionization of an atomic target by a laser pulse depends critically on the laser parameters. In the adiabatic regime, that is, for sufficiently low frequency and high intensity, ionization occurs by tunneling in a static field equal to the momentary value of the laser field [12]. Treating ionization in an oscillating laser field as that in a static field is one of the approximations of the WFAT. The second approximation is that the field amplitude is assumed to be much smaller than the characteristic atomic field, which corresponds to a deep tunneling regime. These conditions on the laser parameters are specified below. The third approximation concerns the description of the target and amounts to the single-active-electron approximation. Under these approximations, Smirnov and Chibisov developed a theory of tunneling ionization of atoms [13]. For decades, the lack of spherical symmetry of one-electron molecular potentials hindered the extension of this theory to molecules. Such an extension became possible in the framework of the method of adiabatic expansion in parabolic coordinates [10,14]. The WFAT developed in Ref. [10] generalizes the results of Ref. [13] to arbitrary molecules. An application of this theory to the analysis of experimental photoelectron spectra of C_2H_4 was demonstrated in Ref. [15]. We mention that another approach to the theory of tunneling ionization was developed in Ref. [16] on the basis of the Keldysh approximation [17]. Other recent theoretical developments for molecules include the semiclassical propagation method [18,19] and a mixed momentum and coordinate space approach [20].

Within the WFAT, the ionization rate as a function of field F is given by an exponential factor multiplied by an asymptotic series in powers of F [10]. The exponential factor rapidly decays as the binding energy of the active orbital grows, so the dominant contribution to tunneling ionization comes from the highest occupied molecular orbital (HOMO). In the leading-order approximation, the dependence of the ionization rate on F factorizes from the dependence on the orientation of the molecule with respect to the field [10]. The field-dependent factor is a simple function of F; the dependence on the orientation is represented by the structure factor for the HOMO. The structure factor does not depend on F and is a property of the HOMO like other related properties, such as polarizability and dipole moment. A peculiarity of this property is that it is determined by the asymptotic behavior of the HOMO at large distances from the molecule. The structure factor for the molecule under investigation is necessary to implement the WFAT. The issue of calculating the molecular structure factors has already been addressed in Ref. [11]. This issue may seem to be technical, but the corresponding techniques must be developed to make the application of the WFAT to particular molecules of current interest possible.

The structure factors can be calculated by quantum chemistry methods. The Hartree-Fock (HF) approximation is central for quantum chemistry approaches to molecular electronic structure calculations and is consistent with the present single-active-electron approximation. There exist different approaches to solving the HF equations numerically. For diatomic molecules, the HF equations can be efficiently solved by a finite-difference grid-based method employing separation of variables in prolate spheroidal coordinates, as implemented in the X2DHF program [21,22]. As shown in Ref. [23], the asymptotic tail of HF orbitals can be accurately obtained by this method. In Ref. [11], the X2DHF program was used to calculate structure factors for the HOMO in a number of diatomic molecules. However, for larger molecules consisting of three and more atoms such a grid-based method is generally not possible because of the difficulty in calculating multicenter integrals. An expansion in a basis set with relatively few basis functions centered on each atom presents an attractive alternative and is indeed the standard approach in modern computational quantum chemistry [24,25]. The basis functions are chosen as Gaussians due to their convenience for calculating multicenter integrals, and Gaussian basis-set HF equations are solved in standard software packages such as GAUSSIAN [26] and GAMESS [27]. Meanwhile, Gaussians decay too rapidly in the asymptotic region. The present work explores the possibility to use Gaussian basis-set quantum chemistry methods to describe the asymptotic tail of the HOMO and hence the possibility to accurately calculate the structure factors for multiatomic molecules.

This paper is organized as follows. In Sec. II, we summarize the formulas defining the tunneling ionization rate and structure factor within the WFAT [10,11]. In Sec. III, we present and discuss our results. To introduce and validate our methodology, we consider a diatomic molecule, CO, for which the structure factors obtained by the grid-based numerical HF [21,22] and the Gaussian basis set [26,27] methods can be compared. Then we investigate the dependence of the asymptotic form of the HOMO on the ionization potential and describe a procedure for extracting the structure factor. At the end of Sec. III, we consider triatomic molecules, CO_2 and OCS, for which a fairly accurate description of the asymptotic tail of the HOMO is obtained using a polarization-consistent Gaussian basis set with optimized exponentials. The conclusions and an outlook are given in Sec. IV.

II. WEAK-FIELD ASYMPTOTIC THEORY

In this section, we summarize the formulas needed to evaluate the tunneling ionization rate from a given HOMO within the WFAT [10]. We choose a geometry where the external electric field $\mathbf{F}$ is always pointing in the positive direction of the z axis of the laboratory frame, so $\mathbf{F} = F\mathbf{e}_z$ with $F > 0$, while the molecule can be rotated with respect to the laboratory frame. Let $\mathbf{r}$ and $\mathbf{r}' = \hat{R}\mathbf{r}$ be the coordinates of the active electron measured from the center of mass of the molecule in the laboratory and a molecular frame, respectively, where $\hat{R}$ describes a rotation from the laboratory to the molecular frame. To find the ionization rate, one needs the field-free energy $E_0 < 0$, orbital $\psi_0(\mathbf{r}')$, and dipole moment $\boldsymbol{\mu}'$ of the HOMO in the molecular frame, where (atomic units are used throughout)

$$\boldsymbol{\mu}' = -\int \psi_0^*(\mathbf{r}')\mathbf{r}'\psi_0(\mathbf{r}')\,d\mathbf{r}'. \tag{1}$$

The corresponding orbital and dipole moment in the laboratory frame are $\psi_0(\hat{R}\mathbf{r})$ and $\boldsymbol{\mu} = \hat{R}^{-1}\boldsymbol{\mu}'$. Here we consider only linear molecules; similar formulas for the general case of nonlinear molecules are summarized in Ref. [11]. For linear molecules, the y' and z' axes of the molecular frame are chosen to coincide with the laboratory y axis and the molecular symmetry axis, respectively. Then the orientation of the molecule is determined by a single angle $\beta \in [0,\pi]$, that between the positive directions of the z and z' axes, and $\hat{R}$ is a rotation about the $y = y'$ axis by this angle.

The ionization rates of atoms and molecules in the single-active-electron approximation can be calculated numerically for arbitrary values of the field F by the method of adiabatic expansion in parabolic coordinates (ξ,η,φ) [10,14,28]. For weak fields satisfying $F \ll F_c$, where F_c is a boundary between the tunneling and overbarrier regimes of ionization, the problem can be treated analytically. The total ionization rate in the weak-field limit is given by [10]

$$\Gamma(\beta) = \sum_{n_\xi=0}^{\infty}\sum_{m=-\infty}^{\infty}\Gamma_{n_\xi m}(\beta) + O(\Gamma^2), \tag{2}$$

where $\Gamma_{n_\xi m}(\beta)$ is the partial rate for ionization into a channel with parabolic quantum numbers n_ξ and m. The asymptotics of $\Gamma_{n_\xi m}(\beta)$ for $F \to 0$ has the form [10]

$$\Gamma_{n_\xi m}(\beta) = |G_{n_\xi m}(\beta)|^2 W_{n_\xi m}(F)[1 + O(F)], \tag{3}$$

where $G_{n_\xi m}(\beta)$ is the *structure factor*,

$$G_{n_\xi m}(\beta) = \lim_{\eta\to\infty} G_{n_\xi m}(\beta,\eta), \tag{4}$$

given by the asymptotic value of the *structure function* [29],

$$G_{n_\xi m}(\beta,\eta) = e^{-\varkappa\mu_z}\eta^{1+|m|/2-Z/\varkappa}e^{\varkappa\eta/2} \times \int_0^\infty\int_0^{2\pi}\phi_{n_\xi|m|}(\xi)\frac{e^{-im\varphi}}{\sqrt{2\pi}}\psi_0(\hat{R}\mathbf{r})\,d\xi\,d\varphi, \tag{5}$$

and $W_{n_\xi m}(F)$ is the *field factor*,

$$W_{n_\xi m}(F) = \frac{\varkappa}{2}\left(\frac{4\varkappa^2}{F}\right)^{2Z/\varkappa-2n_\xi-|m|-1}\exp\left(-\frac{2\varkappa^3}{3F}\right). \tag{6}$$

Here $\varkappa = \sqrt{2|E_0|}$, Z is the charge in the Coulomb tail of the one-electron potential supporting the orbital $\psi_0(\mathbf{r}')$, μ_z is the z component of $\boldsymbol{\mu}$, and $\phi_{n_\xi|m|}(\xi)$ is a parabolic channel function,

$$\phi_{n_\xi|m|}(\xi) = \varkappa^{1/2}(\varkappa\xi)^{|m|/2}e^{-\varkappa\xi/2}\sqrt{\frac{n_\xi!}{(n_\xi+|m|)!}}L_{n_\xi}^{(|m|)}(\varkappa\xi), \tag{7}$$

where $L_n^{(\alpha)}(x)$ are the generalized Laguerre polynomials [30]. As can be seen from Eq. (3), in the leading-order approximation the partial rate $\Gamma_{n_\xi m}(\beta)$ factorizes into two factors, one that depends only on the orientation angle β and one that depends only on the field F. The orientation-dependent structure factor $G_{n_\xi m}(\beta)$ is the most important characteristic which should be extracted from the HOMO. Its dependence on β is contained

in μ_z and $\psi_0(\hat{R}\mathbf{r})$ in Eq. (5). The field factor $W_{n_\xi m}(F)$ is a simple function which depends on the molecule only via Z and $\varkappa$. We note that $G_{n_\xi m}(\beta)$, and hence $\Gamma_{n_\xi m}(\beta)$, are invariant under translations of the coordinate origin of the HOMO [10], as they should be.

The different channels (n_ξ,m) have different powers of F in Eq. (6). In the leading-order approximation, when the correction $O(F)$ in Eq. (3) is neglected, one can retain only the dominant term in Eq. (2), which corresponds to the channel with the smallest values of n_ξ and m. For linear molecules, the unperturbed orbital $\psi_0(\mathbf{r}')$ is characterized by the projection of the electronic angular momentum onto the molecular axis, which is denoted by M. The energy E_0 of the unperturbed state does not depend on the sign of M, so the states with $M \neq 0$ are degenerate. This degeneracy is removed by an arbitrarily weak field, provided that the molecular axis does not coincide with the direction of the field. The correct unperturbed states are certain linear combinations of the two degenerate states [31]. In the present geometry, the molecular axis is rotated by an angle β in the xz plane of the laboratory frame. Then one of these states is even with respect to the xz plane, and the other is odd. The states with $M = 0$ (σ states) belong to the class of even states. For even states, the dominant channel is (0,0), and we have

$$\Gamma_{\text{even}}(\beta) \approx |G_{00}(\beta)|^2 W_{00}(F). \tag{8}$$

For odd states $G_{00}(\beta) = 0$; hence the dominant channels are $(0, \pm 1)$, and we have

$$\Gamma_{\text{odd}}(\beta) \approx 2|G_{01}(\beta)|^2 W_{01}(F). \tag{9}$$

In the particular case of states with $|M| = 1$ (π states), the orbital $\psi_0(\mathbf{r}')$ has a nodal plane. For $\beta = 0$, the nodal plane of an even state coincides with the yz plane, and the nodal plane of an odd state coincides with the xz plane. In this case it is convenient to identify the states by the nodal plane and denote even and odd states by (yz) and (xz), respectively. We will use this notation in Sec. III in the discussion of the results.

The structure factor $G_{n_\xi m}(\beta)$ for the dominant channel as a function of the orientation angle β can be expanded in terms of an appropriate set of standard functions. This helps to compress the information needed for applications and facilitate its exchange between researchers. It is convenient to present $G_{n_\xi m}(\beta)$ in the form [11]

$$G_{n_\xi m}(\beta) = i^p \sum_{l=|M-m|}^{\infty} C^{(l)}_{n_\xi m} \Theta_{l|M-m|}(\beta), \tag{10}$$

where $\Theta_{lm}(\beta)$ is given in terms of the associated Legendre polynomials $P_l^m(x)$ by

$$\Theta_{lm}(\beta) = \sqrt{\frac{(2l+1)(l-m)!}{2(l+m)!}}\, P_l^m(\cos\beta). \tag{11}$$

For even states $M \geqslant 0$, $m \geqslant 0$, and $p = 0$; for odd states $M \geqslant 1$, $m \geqslant 1$ [from $G_{n_\xi 0}(\beta) = 0$ we have $C^{(l)}_{n_\xi 0} = 0$], and $p = 1$. The *structure coefficients* $C^{(l)}_{n_\xi m}$ in expansion (10) can be tabulated for the molecules under investigation and then used for calculating the structure factors $G_{n_\xi m}(\beta)$. Given these coefficients, the application of the WFAT becomes straightforward.

In the preceding discussion, we assumed that the molecule is oriented at a fixed angle β with respect to the field. Although in this work we focus on orientation-resolved structure factors and rates, it is worthwhile to briefly discuss how to apply the WFAT under realistic experimental conditions, where the orientation is never perfect [32]. The ionization rate for a given orientation distribution $P(\beta)$ can be obtained by averaging Eq. (2) over $P(\beta)$. We thus find from Eqs. (8) and (9)

$$\langle\Gamma_{\text{even}}\rangle \approx \langle|G_{00}|^2\rangle W_{00}(F), \quad \langle\Gamma_{\text{odd}}\rangle \approx 2\langle|G_{01}|^2\rangle W_{01}(F), \tag{12}$$

where

$$\langle|G_{n_\xi m}|^2\rangle = \int_0^\pi |G_{n_\xi m}(\beta)|^2 P(\beta) \sin\beta d\beta. \tag{13}$$

The orientation-averaged structure factor (13) for the dominant channel describes tunneling from the HOMO of a partially oriented molecule. This is a characteristic of the molecule that can be determined under realistic experimental conditions.

Finally, we specify the region in the space of laser parameters where the WFAT applies. This region is defined by

$$F \ll F_c \approx \frac{\varkappa^4}{8|2Z - \varkappa(m+1)|}, \quad \omega \ll \frac{F^2}{\varkappa^4}. \tag{14}$$

The first of these conditions guarantees that the laser field amplitude F is much smaller than the critical field F_c for a given channel $(0,m)$, and hence the correction term $O(F)$ in Eq. (3) can be neglected [10,28]. The second condition justifies the adiabatic approximation [12], when ionization in an oscillating laser field $F(t)$ with frequency ω can be treated as that in a static field equal to the momentary value of $F(t)$.

III. RESULTS AND DISCUSSION

To implement the WFAT, the asymptotic behavior of the HOMO $\psi_0(\hat{R}\mathbf{r})$ at large η is needed [see Eqs. (4) and (5)]. We first consider the diatomic CO molecule where grid-based numerical HF (X2DHF) calculations can be performed [21,22]. These calculations are accurate to large η, and the quality of basis-set quantum chemistry calculations using, e.g., GAUSSIAN [26] or GAMESS [27] can be investigated. We then consider the dependence of the asymptotic form on the ionization potential using the examples of atomic He and Be. Then the extraction procedure for obtaining the structure factor is described. Finally, the results for the orientation dependence of the structure factors are shown for CO_2 and OCS. These latter molecules are considered due to the strong current interest stimulated by the existence of conflicting experimental and theoretical data.

A. Convergence studies for the CO molecule

In this section, we use the CO molecule as an example to explore the possibilities for HF calculations performed with a Gaussian basis set to reproduce the asymptotic part of the HOMO. The HOMO of CO has σ symmetry, and according to the discussion in Sec. II, the dominating channel is (0,0). As an accurate reference for the study, we use the results of X2DHF. For CO we use $R = 2.132178$ a.u., and the X2DHF

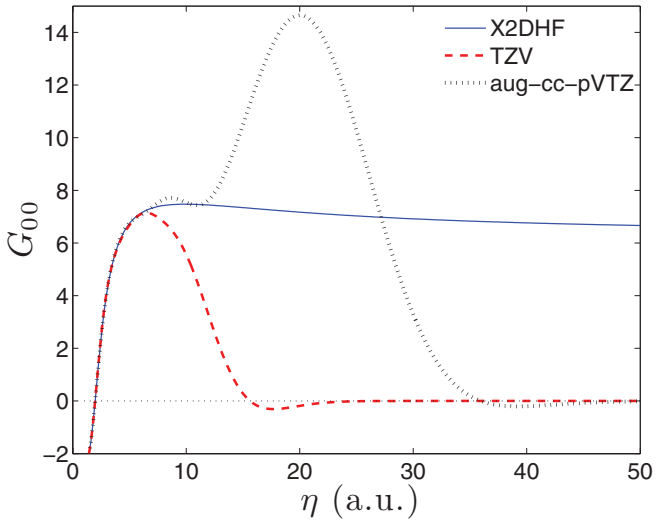

FIG. 1. (Color online) The value of the structure function $G_{00}(\beta = 180°,\eta)$ [see Eq. (5)] as a function of η for the CO HOMO of σ symmetry. The solid blue reference curve uses the HOMO obtained by X2DHF [21,22]. The dashed red curve uses the HOMO from GAUSSIAN [26] with the standard TZV basis set. The dotted black curve uses the HOMO from GAUSSIAN with the standard aug-cc-pVTZ basis set. The nuclei are fixed at the distance $R = 2.132178$ a.u.

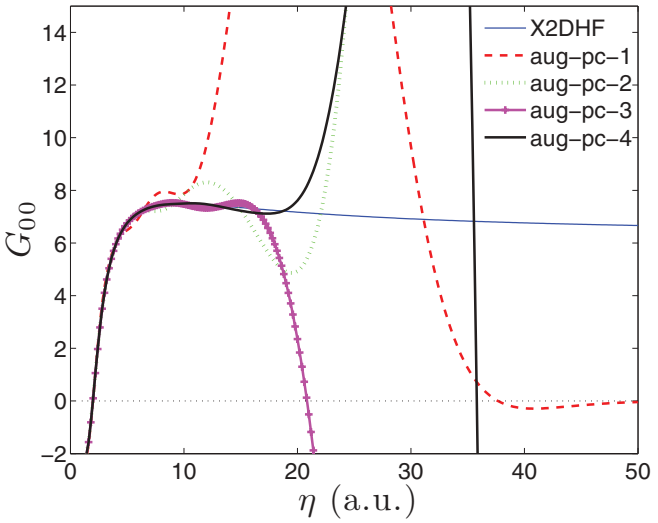

FIG. 2. (Color online) The value of the structure function $G_{00}(\beta = 180°,\eta)$ [see Eq. (5)] for the CO HOMO of σ symmetry. The solid blue reference curve uses the HOMO obtained by X2DHF [21,22]. The dashed red curve uses the HOMO from GAUSSIAN [26] with an aug-pc-1 basis set. The dotted green curve uses the HOMO from GAUSSIAN with a aug-pc-2 basis set. The solid magenta curve with plus signs uses the HOMO from GAUSSIAN with a aug-pc-3 basis set. The solid black curve uses the HOMO from GAUSSIAN with a aug-pc-4 basis set. The nuclei are fixed at the distance $R = 2.132178$ a.u.

calculations give the HOMO energy $E_0 = -0.55493$ a.u., the total energy -112.7908947 a.u., and the dipole moment of the HOMO $\boldsymbol{\mu}' = 1.71735$ a.u., pointing from the C end to the O end in the center of mass.

In the discussion of the results, we first focus on the structure function $G_{n_\xi m}(\beta,\eta)$ defined by Eq. (5). The quality of the asymptotic part of the HOMO obtained using standard Gaussian basis sets is shown in Fig. 1. Figure 1 contains the results for the $G_{00}(\beta = 180°,\eta)$ function based on HOMOs obtained in three different ways: with X2DHF and by expansion in a triple-zeta valence (TZV) [33] and an augmented correlation-consistent triple-zeta (aug-cc-pVTZ) [34,35] standard Gaussian basis set as provided by the built-in basis sets in, e.g., GAUSSIAN and GAMESS [26,27]. It is seen that the TZV and aug-cc-pVTZ follow the X2DHF result only up to $\eta \simeq 5$ a.u. The TZV result drops off rapidly and approaches a vanishing value for G_{00} which is far from the accurate result of the X2DHF calculation. The rapidly vanishing value for G_{00} reflects that Gaussian basis functions fall off too rapidly and are unable to describe the asymptotic part of the HOMO. The aug-cc-pVTZ result, on the other hand, provides G_{00} values that oscillates around the reference value up to $\eta \simeq 10$ a.u.

The requirement for an accurate representation of the asymptotic region of the HOMO (and the aug-cc-pVTZ result) suggests that basis sets augmented with diffuse functions should be used. The polarization-consistent basis sets have been optimized for density-functional theory, which have very similar basis-set requirements as HF, and are available in five different quality levels from (unpolarized) double-zeta to (polarized) pentuple-zeta quality (pc-n, $n = 0$–4) [36] and with the option of augmenting with diffuse functions (aug-pc-n) [37]. It has been shown that these basis sets are capable of reproducing grid-based numerical HF energies for diatomic systems to micro-Hartree accuracy [38]. It was thus anticipated that they should provide a systematic way of approaching the X2DHF results.

In the following calculations, all basis sets have been used in their uncontracted forms. Analytical gradients of the HF energy with respect to basis-function exponents have been calculated with the DALTON program [39]. Basis exponent optimizations have been done using a pseudo-Newton-Raphson method. Starting values were taken from the standard pc-n basis sets [36].

The results using the uncontracted versions of the aug-pc-n ($n = 1,2,3,4$) basis sets are shown in Fig. 2. While there clearly is a systematic improvement as the basis-set quality is increased, it is also evident that erratic oscillations occur for large η values for all the basis sets. The regular (unaugmented) pc-n basis sets also display oscillations, although not as pronounced (not shown). The origin of this oscillatory behavior was traced to the fact that the molecular orbitals are expanded in a basis set with fixed (predetermined) exponent values for each basis function optimized for the individual atoms. The nonconvergent nature of the G_{00} value as the size of the basis set is increased is unusual, as essentially all contemporary electronic structure calculations using Gaussian basis functions employ basis sets with fixed exponent values, and it is generally agreed that this provides a robust method for calculating a large variety of properties [24,25]. For this particular property, however, the use of standard basis sets causes problems, which can be understood as follows. For a given quality basis set, the resulting HF wave function approximates the grid-based numerical HF result to a given accuracy, which can be quantified by how close the total energy

is to the value of the latter approach. A basis set capable of reproducing the grid-based HF energy to within (say) 10^{-3} a.u. will provide a correspondingly accurate wave function in the region where the wave function contributes at least by 10^{-3} a.u. in terms of energy, which corresponds to an η value of (say) 10 a.u. The variational procedure for determining the basis-function coefficients will ensure the optimum linear combinations of all basis functions in this energy-important region. The asymptotic behavior is determined exclusively by the most diffuse basis functions (smallest exponents), but their coefficients are determined by their energy contribution in the energy-important core-valence region. Any fixed exponent basis set will be (slightly) nonoptimum for the particular molecular system, and the most diffuse basis functions may thus serve to patch deficiencies in the remaining basis set in the core-valence region, and this leads to erratic behavior in the asymptotic region.

The above analysis suggests that it should be possible to achieve a stable and systematic convergence of the structure function $G_{00}(\beta,\eta)$ to the grid-based numerical HF result by employing a sequence of basis sets where all exponents are fully (variationally) optimized with respect to the total energy. This procedure is illustrated in Fig. 3. In addition to results from exponent-optimized versions of the pc-n ($n = 1,2,3,4$) basis sets, we have included results from a pc-5-type basis set which is $22s14p8d5f3g2h1i$ in composition [38]. The total energies are 7×10^{-2}, 4×10^{-3}, 1×10^{-4}, 9×10^{-6}, and 1×10^{-7} a.u. above the X2DHF value, respectively. As the basis set approaches the grid-based numerical HF limit in an energetic sense, the outermost basis function exponents gradually become smaller. This reflects that a closer agreement with the grid-based numerical HF energy requires a better representation of the orbital at larger distances. There is thus a clear correlation between the energy convergence and how far out the asymptotic region of the wave function is accurate. Furthermore, with the optimized exponents the prediction of the structure factor at larger η decays smoothly to zero, rather than displaying erratic oscillations. The former just reflects that Gaussian functions decay too fast compared to the correct exponential asymptotic behavior displayed by the grid-based approach.

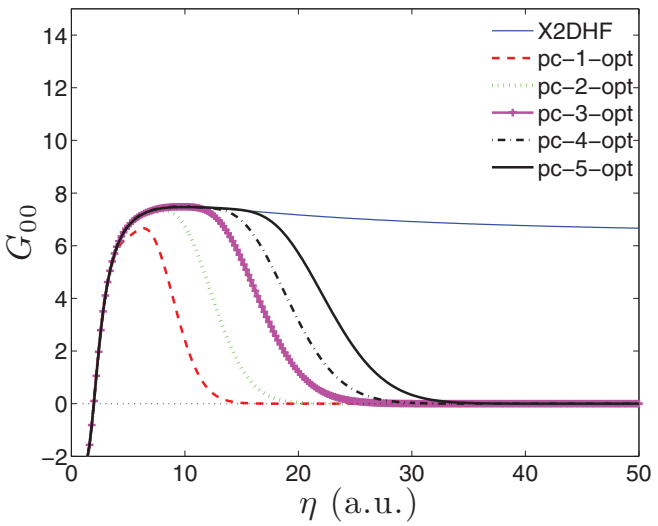

FIG. 3. (Color online) The value of the structure function $G_{00}(\beta = 180°,\eta)$ [see Eq. (5)] as a function of η for the CO HOMO of σ symmetry. The solid blue reference curve uses the HOMO obtained by X2DHF [21,22]. The dashed red curve uses the HOMO from GAUSSIAN [26] with an optimized pc-1 basis set. The dotted green curve uses the HOMO from GAUSSIAN with an optimized pc-2 basis set. The solid magenta curve with plus signs uses the HOMO from GAUSSIAN with an optimized pc-3 basis set. The dot-dashed black curve uses the HOMO from GAUSSIAN with an optimized pc-4 basis set. The solid black curve uses the HOMO from GAUSSIAN with an optimized pc-5 basis set. The nuclei are fixed at the distance $R = 2.132178$ a.u.

B. Dependence on ionization potential

The asymptotic region of the HOMO should display an exponential decay. Basis sets that produce the same accuracy in terms of energy relative to the HF limit for systems with different ionization potentials should thus display an accurate large-η behavior to different maximum η values. This is shown in Figs. 4 and 5 for the He and Be atoms with four different optimized basis sets producing energies within 10^{-2}, 10^{-4}, 10^{-6}, and 10^{-8} a.u. of the corresponding HF limits. The HOMO energies are -0.918 a.u. and -0.309 a.u., and Eq. (5) indicates that the maximum η value for a given energy accuracy should be related by a factor $\sqrt{0.918/0.309} \simeq 1.7$. This is indeed observed in Figs. 4 and 5.

The combination of Figs. 3, 4, and 5 shows that the use of basis sets that are fully optimized with respect to basis-function exponents produces reliable behavior for the structure factor out to a well-defined maximum η value. The use of standard fixed exponent basis sets will, in general, produce unpredictable results at moderate to large η. The performance

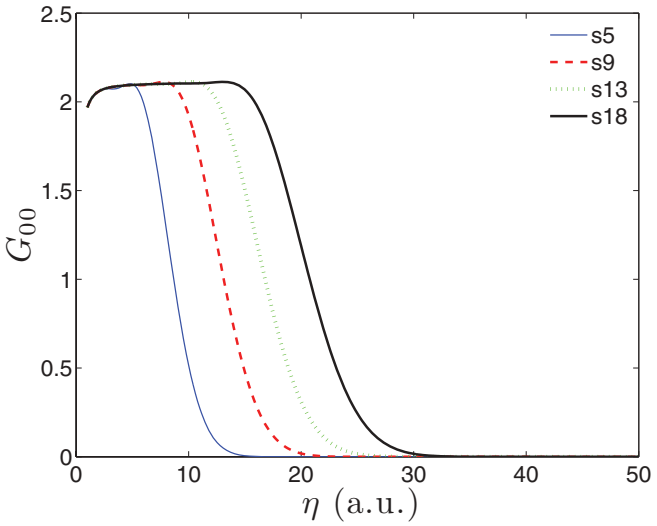

FIG. 4. (Color online) The value of the structure function $G_{00}(\eta)$ [see Eq. (5)] as a function of η for the $1s$ electron in the He atom. The solid blue curve uses the HOMO from GAUSSIAN [26] with a basis with 5 s orbitals. The dashed red curve uses the HOMO from GAUSSIAN with a basis with 9 s orbitals. The dotted green curve uses the HOMO from GAUSSIAN with a basis with 13 s orbitals. The solid black curve uses the HOMO from GAUSSIAN with a basis with 18 s orbitals.

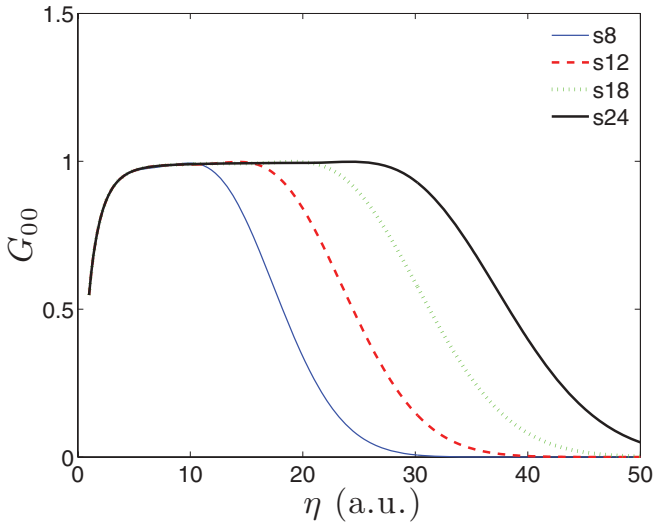

FIG. 5. (Color online) The value of the structure function $G_{00}(\eta)$ [see Eq. (5)] as a function of η for the $2s$ electron in the Be atom. The solid blue curve uses the HOMO from GAUSSIAN [26] with a basis with 8 s orbitals. The dashed red curve uses the HOMO from GAUSSIAN with a basis with 12 s orbitals. The dotted green curve uses the HOMO from GAUSSIAN with a basis with 18 s orbitals. The solid black curve uses the HOMO from GAUSSIAN with a basis with 24 s orbitals.

for a given system will depend on how close the standard exponent values are to the fully optimized ones, but since these are system dependent, the same basis set will produce results of different quality for different systems. Employing basis sets with molecule-specific optimized exponents will secure a monotonic improvement with increasing basis size. In the following we will use the most accurate pc-n ($n = 4,5$) results to extract the value of the structure factor.

C. Extraction of the structure factor and results for CO

In this section, the procedure for the extraction of the structure factor is described using the example of CO where accurate grid-based X2DHF results are available. We fix β and expand the structure function $G_{n_\xi m}(\beta,\eta)$ of Eq. (5) as a polynomial in $1/\eta$ and consider the asymptotic expansion

$$G_{n_\xi m}(\beta,\eta) = G_{n_\xi m}(\beta) + \sum_{j=1}^{n} c_j^{(n_\xi m)}(\beta)\left(\frac{1}{\eta}\right)^j, \qquad (15)$$

where the leading-order constant term $G_{n_\xi m}(\beta)$ is the structure factor of Eq. (4) for the orientation β of the molecule with respect to the field. It is seen from Figs. 1–3 that there is an extended η region with a stable value of $G_{00}(\beta,\eta)$ for the X2DHF results, and we choose 20 sampling points in the range of $\eta \in [20;70]$ a.u. to fit the structure function with the asymptotic polynomial expansion in Eq. (15) for $n = 1,\ldots,7$. The result of this procedure is shown in Fig. 6 by the flat curve with circles. The point corresponding to $n = 0$ is obtained as the G_{00} value at $\eta = 70$ a.u. The minor variation in the result for $G_{00}(\beta,\eta)$ with changing n is an indication of a well-converged result.

Turning to the results obtained using the HOMO from the Gaussian basis-set calculation, we see from Fig. 3 that even

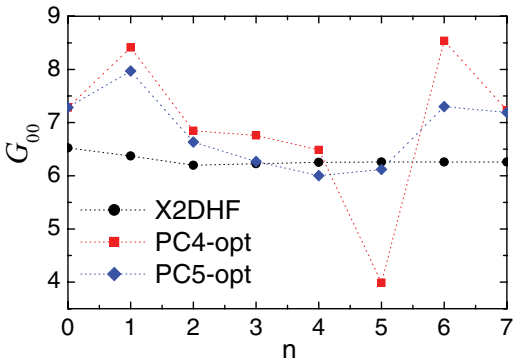

FIG. 6. (Color online) The dependence of the structure factor $G_{00}(\beta)$ [see Eq. (4)] on the method used to obtain the HOMO of CO (X2DHF [21,22], circles; GAUSSIAN [26] with an optimized pc-4 basis set, squares; and an optimized pc-5, diamonds) and the order n of the polynomial in $1/\eta$ [see Eq. (15)] in the asymptotic expansion.

the most accurate basis set only covers an η range up to 15 a.u. before a drop-off related to the Gaussian basis occurs. We illustrate the associated problems considering only the most accurate pc-4 and pc-5 basis sets. As indicated by the curves in Fig. 3, for the pc-4 HOMO the range $\eta \in [5;10]$ a.u. can be used, while for the pc-5 HOMO the range $\eta \in [5;15]$ a.u. can be used for the fit to Eq. (15). As shown by the scattering of the squares and diamonds in Fig. 6, the pc-4 and pc-5 results obtained in this way are quite sensitive to the order of the expansion, in contrast to the grid-based result. The problem stems from the much narrower plateau-like interval available for fitting. Based on the spirit of an asymptotic expansion, we therefore choose to fit with only the constant term in the expansion in Eq. (15) by taking the value of the structure function $G_{00}(\beta,\eta)$ at the maximum η with coinciding pc-4 and pc-5 results. This procedure, i.e., taking the $G_{00}(\beta)$ value at the maximum η where the pc-$(n-1)$ and the pc-n results coincide, will be followed below for the HF calculations with Gaussian basis sets for CO_2 and OCS.

We now turn to a discussion of the orientation dependence of the tunneling ionization rate using the outlined procedure. In Fig. 7 we show the orientation dependence of the structure factor $|G_{00}(\beta)|^2$ for the (0,0) channel for CO using the X2DHF HOMO and the optimized pc-4 and pc-5 Gaussian basis sets. The agreement between the pc-4 and pc-5 results is satisfying, while there is a deviation at the quantitative level between these and the X2DHF results. We find, as in previous studies [11], that ionization occurs most likely when the field points from the O end to the C end. This prediction of the WFAT is opposite to what is observed experimentally [40–42]. The experiment in Ref. [42], however, was carried out with a central wave length of 790 nm and for peak intensities between 4×10^{14} and 2×10^{15} W/cm^2. These laser parameters place the experimental conditions outside the validity range of the WFAT [see Eq. (14)], and the disagreement shows that it is necessary for theory to consider higher-order effects in the field.

In Table I, we give the structure coefficients [see Eq. (10)] obtained by the fitting procedure applied to the X2DHF HOMO of CO. The values for $C_{00}^{(l)}$ are slightly different from the values given in Table IV of Ref. [11], where the fitting was performed including only up to linear order, $n = 1$ in the expansion of

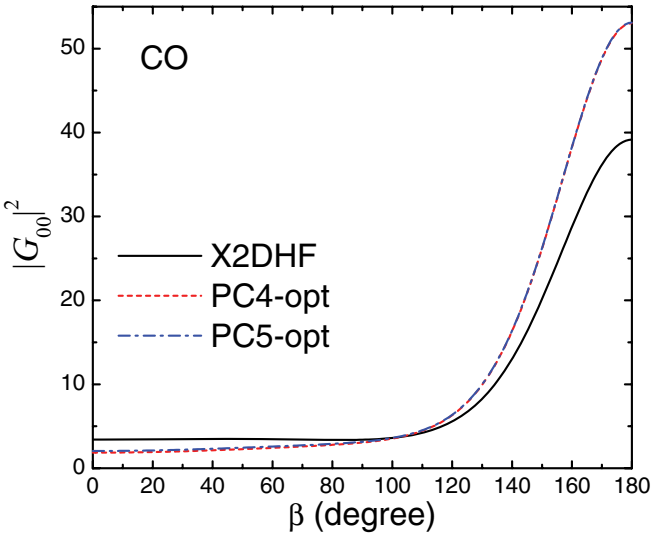

FIG. 7. (Color online) The dependence of the structure factor on the angle β between the internuclear axis and the electric field for the HOMO in CO of σ symmetry. The C (O) atom is on the negative (positive) z axis in the molecular fixed frame. The solid black curve uses the HOMO wave function obtained by X2DHF [21,22]. The dashed red curve uses the HOMO from GAUSSIAN [26] with an optimized pc-4 basis set. The dot-dashed blue curve uses the HOMO from GAUSSIAN with an optimized pc-5 basis set. The nuclei are fixed at the distance $R = 2.132178$ a.u.

Eq. (15). The results for the orientation dependence of G_{00} with the present and the previous [11] structure coefficients from the X2DHF calculation cannot be discriminated on the scale of the figure, but the present set is more accurate and is included for future reference.

D. Results for OCS and CO_2

Having established that fully optimized Gaussian basis sets are capable of reproducing the correct asymptotic behavior of the HOMO to useful η values, we applied the same methodology for the CO_2 and OCS molecules, where experimental data are available but where grid-based numerical HF results are not. For these molecules we use the HF

TABLE I. Structure coefficients [see Eq. (10)] for the HOMO of CO of σ symmetry ($R = 2.132178$ a.u., $E_0 = -0.55493$ a.u., $\mu' = 1.72735$ a.u.) obtained from the X2DHF HOMO [21,22]. $a[b] = a^b$.

l	$C_{00}^{(l)}$
0	3.347
1	−1.002
2	0.821
3	−0.458
4	0.169
5	−0.479[−1]
6	0.113[−1]
7	−0.227[−2]
8	0.398[−3]
9	−0.620[−4]
10	0.866[−5]

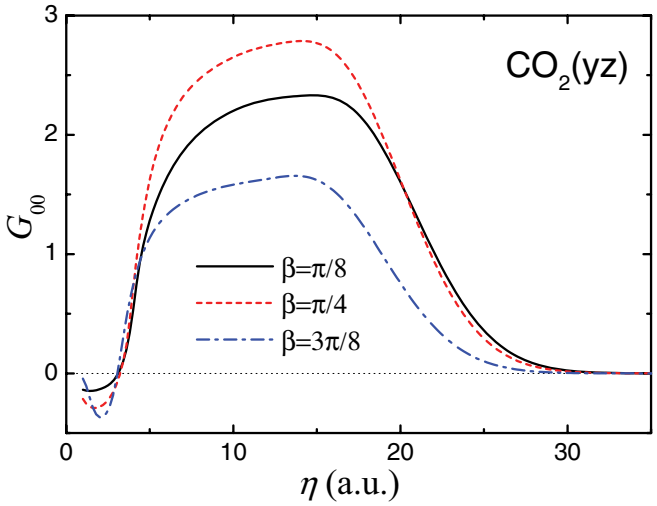

FIG. 8. (Color online) The value of the structure function $G_{00}(\beta,\eta)$ [see Eq. (5)] as a function of η for the $CO_2(yz)$ HOMO of π_g symmetry and for three different orientations β of the internuclear axis with respect to the direction of the electric field using the HOMO obtained by GAUSSIAN [26] with the optimized pc-4 basis set. The distance from C to O is $R = 2.19605$ a.u.

results with the optimized exponents in the pc-4 basis set. For CO_2 (distance from C to O $R = 2.19605$ a.u.) the HOMO energy is $E_0 = -0.54490$ a.u. For OCS (z'[O] $= -3.19847$ a.u., z'[C] $= -0.98957$ a.u., z'[S] $= 1.97032$ a.u.) the HOMO energy is $E_0 = -0.42178$ a.u., and the dipole of the HOMO is $\boldsymbol{\mu}' = -0.88069$ a.u. and points from the S end to the O end, in agreement with previous findings [43–45].

Figures 8 and 9 show the $G_{00}(\beta,\eta)$ function for different values of β for the $CO_2(yz)$ and the OCS(yz) orbitals of π_g and π symmetry, respectively. The value used for the structure

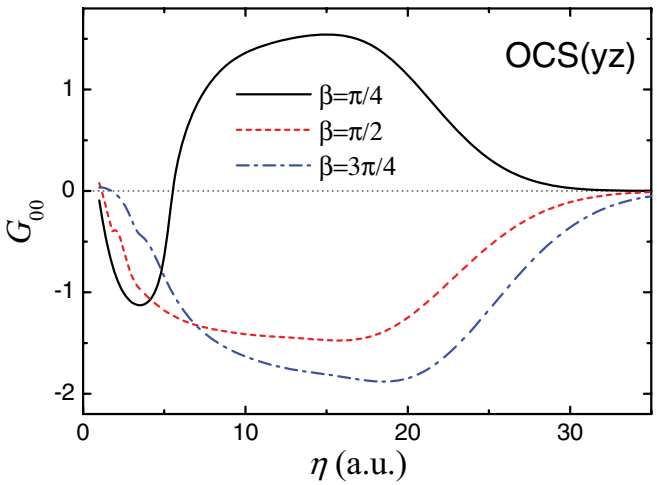

FIG. 9. (Color online) The value of the structure function $G_{00}(\beta,\eta)$ [see Eq. (5)] as a function of η for the OCS(yz) HOMO of π symmetry and for three different orientations β of the internuclear axis with respect to the direction of the electric field using the HOMO obtained by GAUSSIAN [26] with the optimized pc-4 basis set. The O (S) atom is on the negative (positive) z' axis in the molecular fixed frame. z'[O] $= -3.19847$ a.u., z'[C] $= -0.98957$ a.u., z'[S] $= 1.97032$ a.u.

TABLE II. Structure coefficients for the HOMO of CO_2 of π_g symmetry (distance from C to O $R = 2.19605$ a.u., $E_0 = -0.54490$ a.u.) and for the HOMO of OCS of π symmetry at $z'[\mathrm{O}] = -3.19847$ a.u., $z'[\mathrm{C}] = -0.98957$ a.u., and $z'[\mathrm{S}] = 1.97032$ a.u. ($E_0 = -0.42178$ a.u., $\mu' = -0.88069$ a.u.) obtained using GAUSSIAN [26] with an optimized pc-4 basis set. $a[b] = a^b$.

l	$C_{00}^{(l)}$ [$CO_2(yz)$]	$C_{01}^{(l)}$ [$CO_2(xz)$]	$C_{00}^{(l)}$ [OCS(yz)]	$C_{01}^{(l)}$ [OCS(xz)]
0				−0.762
1		4.419	−1.093	3.038
2	2.658		1.470	1.471
3		0.518	0.690	0.757
4	0.294		0.352	0.268
5		0.202[−1]	0.123	0.759[−1]
6	0.116[−1]		0.340[−1]	0.164[−1]
7		−0.696[−4]	0.749[−2]	0.147[−2]
8	0.156[−3]		0.105[−2]	
9			−0.317[−3]	

factor is obtained as discussed in connection with Fig. 6, and the values for the structure coefficients are given in Table II. Based on the comparison between the X2DHF and the basis-set HF results in the CO case, we estimate the structure factor for these triatomics to have an error of ∼10%, which is a significant improvement compared to existing technology using HF calculations and conventional TZV or aug-cc-pVTZ basis sets.

Figure 10 shows the dependence of the structure factor for CO_2 in the dominating (0,0) channel for the $CO_2(yz)$ HOMO and in the dominating (0,1) channel for the $CO_2(xz)$ HOMO. The double-peaked structure in the dominating (0,0) channel is characteristic for a molecule with π symmetry. The minima at $\beta = \{0^\circ, 180^\circ\}$ and $\beta = 90^\circ$ in this channel are due to nodal planes along and perpendicular to the molecular axis, respectively. Note that in order to obtain the orientation-dependent channel-specific tunneling ionization rate of Eq. (3), the structure factors in Fig. 10 (and in Fig. 11 below) should be multiplied by the field factor $W_{0m}(F)$ of Eq. (6). Since $W_{01}(F) = [F/(4\kappa^2)]W_{00}(F)$ and the factor $F/(4\kappa^2) \ll 1$ in the weak-field limit for typical values of κ, this multiplication results in a suppression of Γ_{01} compared to Γ_{00} for nonvanishing G_{00} (see also the discussion in Ref. [11]).

The CO_2 molecule has attracted attention since experiments appeared showing that the rate peaks at $\beta = 45^\circ$ [46,47]. In contrast the molecular Ammosov-Delone-Krainov (MO-ADK) result [48] predicted a peak at around $\simeq 25^\circ$ [46] or $\beta \simeq 33^\circ$ [49–52] depending on the procedure used for the extraction of the asymptotic properties used for the evaluation of the tunneling rate, while a tunneling theory based on a mixed position and momentum space approach predicts $\beta \simeq 45^\circ$ [20]. Another approach to the tunneling problem based on semiclassical propagation of the HOMO from a surface and to large distances was considered in Refs. [18,19] and provided

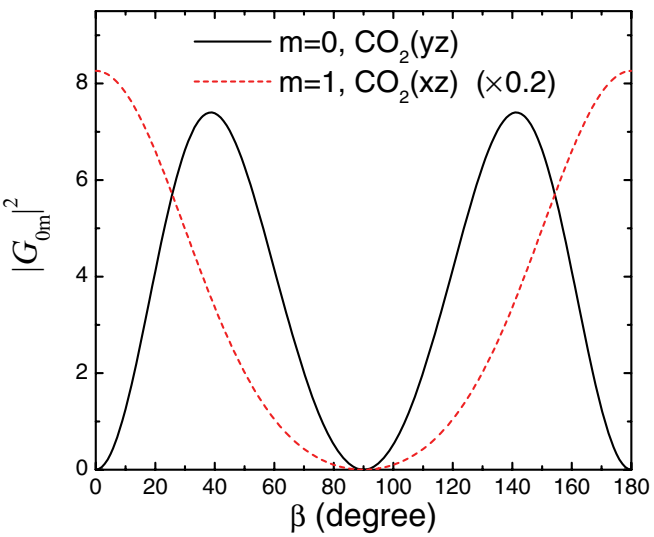

FIG. 10. (Color online) The dependence of the structure factors on the angle β between the internuclear axis and the electric field for the two degenerate HOMOs in CO_2 of π_g symmetry. $CO_2(yz)$ [$CO_2(xz)$] denotes that the nodal plane of the π orbital is in the yz (xz) plane. Solid black curve, $m = 0$; dashed red curve, $m = 1$. The distance from C to O is $R = 2.19605$ a.u.

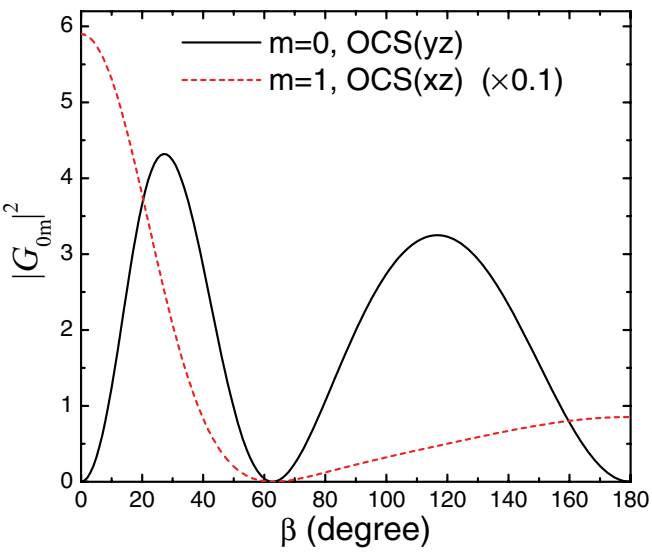

FIG. 11. (Color online) The dependence of the structure factors on the angle β between the internuclear axis and the electric field for the two degenerate HOMOs in OCS of π_g symmetry. OCS(yz) [OCS(xz)] denotes that the nodal plane of the π orbital is in the yz (xz) plane. Solid black curve, $m = 0$; dashed red curve, $m = 1$. The O (S) atom is on the negative (positive) z' axis in the molecular fixed frame. $z'[\mathrm{O}] = -3.19847$ a.u., $z'[\mathrm{C}] = -0.98957$ a.u., $z'[\mathrm{S}] = 1.97032$ a.u.

a maximum in the rate for CO_2 for $\beta \simeq 25°$–$30°$ [19]. In Ref. [11], using an aug-cc-pVTZ basis, a maximum in the rate was found at $\sim 32°$. With the current pc-4 basis set giving an improved description of the asymptotic form of the HOMO, we find a maximum in the rate at $\simeq 39°$. This variation reflects the sensitivity of the WFAT to the quality of the asymptotic form of the HOMO. We note that CO_2 has also been considered theoretically by solving the time-dependent Schrödinger equation (TDSE) in various approximations, and also in this case no clear conclusion can be drawn: TDSE results within the single-active-electron approximation predicted $\beta \simeq 45°$ [53], multiple-orbital TDSE calculations predicted $\beta \simeq 40°$ [54], the multielectron TDSE approach predicted $\beta \simeq 35°$ [55], and a time-dependent density-functional theory calculation predicted $\beta \simeq 40°$ [56]. Recent experimental results indicate that contributions from lower-lying orbitals may be involved [57].

Figure 11 shows the orientation dependence of the structure factor in the dominating channel for OCS(yz) [(0,0) channel] and for OCS(xz) [(0,1) channel] obtained with the pc-4 basis set. Focusing on the main contribution to the rate [the (0,0) channel], we see three minima at $\beta = 0°, 61°$, and $180°$. These are due to the nodal plane along the internuclear distance and a nodal cone at around $61°$ for the HOMO of π symmetry. The maximum in the signal is at $\simeq 27°$, where the dipole of the HOMO (pointing from the S end to the O end) has a component antiparallel to the direction of the field, and the ionization potential of the HOMO is decreased by the Stark shift, $-\boldsymbol{\mu} \cdot \mathbf{F}$. For the orientations with $\beta \in [90°; 180°]$ the dipole of the HOMO has a component parallel with the field, and the ionization potential is increased by the Stark shift. The result in Fig. 11 shows that the OCS molecule ionizes most readily when the dipole of the HOMO has a component antiparallel to the field direction, i.e., when the electron that tunnels leaves from the O end in the direction opposite to the field. This finding is consistent with previous combined experimental and theoretical work on strong-field ionization of OCS in circularly polarized fields [43,44,58]. For strong-field ionization by linearly polarized pulses the experimental result for the alignment-dependent ionization yield in OCS shows a maximum when the ionizing field is perpendicular to the internuclear axis [45]. Figure 11 shows that this finding contrasts the prediction of the WFAT. One possible reason for this difference lies in the role of excited states. As discussed in Ref. [45], it is expected that excited states are more readily populated in linearly polarized fields than in circularly polarized fields. Ionization taking place through excited states will modify the orientation-dependent yield, as seen, e.g., in TDSE calculations within the single-active-electron approximation in CO_2 [53]. Disagreement between photoelectron angular distributions and theory for strong-field ionization of the CS_2 molecule in linearly polarized fields was previously attributed to the participation of excited states in the ionization dynamics [59].

IV. CONCLUSION AND OUTLOOK

We find that it is possible to calculate the asymptotic behavior of the wave function in the form of the HOMO for HF wave functions with Gaussian basis functions for expanding the molecular orbitals, such that a reasonable accuracy can be obtained for extracting structure factors. A calibration study for the CO molecule, where grid-based numerical HF results are available, unexpectedly showed that it is necessary to employ basis functions with exponents that are fully optimized with respect to the energy in order to obtain stable results. By using a hierarchical sequence of fully optimized basis sets, it is possible to calculate structure factors for molecular systems in general, as illustrated by the results for CO_2 and OCS [60]. The main computational problem for expanding the methodology to larger systems is the necessity to fully optimize all exponents of basis sets of at least pentuple-zeta quality, which is a large nonlinear optimization problem. This challenge can, however, be dealt with and the present work therefore outlines an accurate methodology that can be extended to general molecules. In particular the tunneling rates of the WFAT will be useful for the description of the tunneling step in laser-induced scattering spectroscopy of larger molecules where much less is known about dynamics and correlations out of equilibrium.

ACKNOWLEDGMENTS

This work was supported by grants from the Danish Center for Scientific Computation, the Danish Natural Science Research Council, the Aarhus University Research Foundation, and an ERC-StG (Project No. 277767-TDMET). O.I.T. thanks the Russian Foundation for Basic Research for support through Grant No. 11-02-00390-a. T.M. acknowledges the support of Grants-in-Aid for scientific research (B) and (C) from the Japan Society for the Promotion of Science.

[1] F. Krausz and M. Ivanov, Rev. Mod. Phys. **81**, 163 (2009).
[2] C. D. Lin, A.-T. Le, Z. Chen, T. Morishita, and R. Lucchese, J. Phys. B **43**, 122001 (2010).
[3] P. Eckle, A. N. Pfeiffer, C. Cirelli, A. Staudte, R. Dörner, H. G. Muller, M. Böttiker, and U. Keller, Science **322**, 1525 (2008).
[4] A. N. Pfeiffer, C. Cirelli, M. Smolarski, D. Dimitrovski, M. Abu-samha, L. B. Madsen, and U. Keller, Nat. Phys. **8**, 76 (2012).
[5] N. I. Shvetsov-Shilovski, D. Dimitrovski, and L. B. Madsen, Phys. Rev. A **85**, 023428 (2012).
[6] T. Morishita, A.-T. Le, Z. Chen, and C. D. Lin, Phys. Rev. Lett. **100**, 013903 (2008).
[7] T. Morishita, M. Okunishi, K. Shimada, G. Prümper, Z. Chen, S. Watanabe, K. Ueda, and C. D. Lin, J. Phys. B **42**, 105205 (2009).
[8] J. Maurer, D. Dimitrovski, L. Christensen, L. B. Madsen, and H. Stapelfeldt, Phys. Rev. Lett. **109**, 123001 (2012).
[9] A.-T. Le, T. Morishita, R. R. Lucchese, and C. D. Lin, Phys. Rev. Lett. **109**, 203004 (2012).

[10] O. I. Tolstikhin, T. Morishita, and L. B. Madsen, Phys. Rev. A **84**, 053423 (2011).
[11] L. B. Madsen, O. I. Tolstikhin, and T. Morishita, Phys. Rev. A **85**, 053404 (2012).
[12] O. I. Tolstikhin and T. Morishita, Phys. Rev. A **86**, 043417 (2012).
[13] B. M. Smirnov and M. I. Chibisov, Zh. Eksp. Teor. Fiz. **49**, 841 (1965) [Sov. Phys. JETP **22**, 585 (1966)].
[14] P. A. Batishchev, O. I. Tolstikhin, and T. Morishita, Phys. Rev. A **82**, 023416 (2010).
[15] C. Wang, M. Okunishi, R. R. Lucchese, T. Morishita, O. I. Tolstikhin, L. B. Madsen, K. Shimada, D. Ding, and K. Ueda, J. Phys. B **45**, 131001 (2012).
[16] A. M. Perelomov, N. B. Popov, and M. V. Terent'ev, Zh. Eksp. Teor. Fiz. **50**, 1393 (1966) [Sov. Phys. JETP **23**, 924 (1966)].
[17] L. V. Keldysh, Zh. Eksp. Teor. Fiz. **47**, 1945 (1964) [Soc. Phys. JETP **20**, 1307 (1965)].
[18] I. I. Fabrikant and G. A. Gallup, Phys. Rev. A **79**, 013406 (2009).
[19] G. A. Gallup and I. I. Fabrikant, Phys. Rev. A **81**, 033417 (2010).
[20] R. Murray, M. Spanner, S. Patchkovskii, and M. Y. Ivanov, Phys. Rev. Lett. **106**, 173001 (2011).
[21] J. Kobus, L. Laaksonen, and D. Sundholm, Comput. Phys. Commun. **98**, 346 (1996).
[22] http://www.leiflaaksonen.eu/num2d.html.
[23] T. K. Kjeldsen and L. B. Madsen, Phys. Rev. A **71**, 023411 (2005).
[24] F. Jensen, *Introduction to Computational Chemistry* (Wiley, New York, 2007).
[25] T. Helgaker, P. Jørgensen, and J. Olsen, *Molecular Electronic-Structure Theory* (Wiley, New York, 2000).
[26] M. J. Frisch, G. W. Trucks, H. B. Schlegel, G. E. Scuseria, M. A. Robb, J. R. Cheeseman, G. Scalmani, V. Barone, B. Mennucci, G. A. Petersson *et al.*, GAUSSIAN 09, Revision A.1, gaussian Inc., Wallingford, CT, 2009.
[27] M. W. Schmidt, K. K. Baldridge, J. A. Boatz, S. T. Elbert, M. S. Gordon, J. H. Jensen, S. Koseki, N. Matsunaga, K. A. Nguyen, S. Su *et al.*, J. Comput. Chem. **14**, 1347 (1993).
[28] L. Hamonou, T. Morishita, and O. I. Tolstikhin, Phys. Rev. A **86**, 013412 (2012).
[29] There is a misprint in the corresponding formulas in Refs. [11, 28]: the square-root factor in the first line of Eq. (7) and Eq. (59) therein, respectively, should be omitted.
[30] *Handbook of Mathematical Functions*, edited by M. Abramowitz and I. A. Stegun (Dover, New York, 1972).
[31] L. D. Landau and E. M. Lifschitz, *Quantum Mechanics (Non-relativistic Theory)* (Pergamon, Oxford, 1977).
[32] H. Stapelfeldt and T. Seideman, Rev. Mod. Phys. **75**, 543 (2003).
[33] T. H. Dunning, J. Chem. Phys. **55**, 716 (1971).
[34] T. H. Dunning, Jr., J. Chem. Phys. **90**, 1007 (1989).
[35] R. A. Kendall, T. H. Dunning, Jr., and R. Harrison, J. Chem. Phys. **96**, 6796 (1992).
[36] F. Jensen, J. Chem. Phys. **115**, 9113 (2001).
[37] F. Jensen, J. Chem. Phys. **117**, 9234 (2002).
[38] F. Jensen, Theor. Chem. Acc. **113**, 267 (2002).
[39] C. Angeli, K. L. Bak, V. Bakken, O. Christiansen, R. Cimiraglia, S. Coriani, P. Dahle, E. K. Dalskov, T. Enevoldsen, B. Fernandez *et al.*, DALTON, a molecular electronic structure program, release dalton2011, 2011; see http://daltonprogram.org.
[40] H. Ohmura, N. Saito, and T. Morishita, Phys. Rev. A **83**, 063407 (2011).
[41] H. Li, D. Ray, S. De, I. Znakovskaya, W. Cao, G. Laurent, Z. Wang, M. F. Kling, A. T. Le, and C. L. Cocke, Phys. Rev. A **84**, 043429 (2011).
[42] J. Wu, L. P. H. Schmidt, M. Kunitski, M. Meckel, S. Voss, H. Sann, H. Kim, T. Jahnke, A. Czasch, and R. Dörner, Phys. Rev. Lett. **108**, 183001 (2012).
[43] L. Holmegaard, J. L. Hansen, L. Kalhøj, S. L. Kragh, H. Stapelfeldt, F. Filsinger, J. Küpper, G. Meijer, D. Dimitrovski, M. Abu-samha *et al.*, Nat. Phys. (London) **6**, 428 (2010).
[44] D. Dimitrovski, M. Abu-samha, L. B. Madsen, F. Filsinger, G. Meijer, J. Kuepper, L. Holmegaard, L. Kalhoj, J. H. Nielsen, and H. Stapelfeldt, Phys. Rev. A **83**, 023405 (2011).
[45] J. L. Hansen, L. Holmegaard, J. H. Nielsen, H. Stapelfeldt, D. Dimitrovski, and L. B. Madsen, J. Phys. B **45**, 015101 (2012).
[46] D. Pavičić, K. F. Lee, D. M. Rayner, P. B. Corkum, and D. M. Villeneuve, Phys. Rev. Lett. **98**, 243001 (2007).
[47] I. Thomann, R. Lock, V. Sharma, E. Gagnon, S. T. Pratt, H. C. Kapteyn, M. M. Murnane, and W. Li, J. Phys. Chem. A **112**, 9382 (2008).
[48] X. M. Tong, Z. X. Zhao, and C. D. Lin, Phys. Rev. A **66**, 033402 (2002).
[49] S.-F. Zhao, C. Jin, A.-T. Le, T. F. Jiang, and C. D. Lin, Phys. Rev. A **80**, 051402 (2009).
[50] S.-F. Zhao, C. Jin, A.-T. Le, T. F. Jiang, and C. D. Lin, Phys. Rev. A **81**, 033423 (2010).
[51] S.-F. Zhao, C. Jin, A.-T. Le, and C. D. Lin, Phys. Rev. A **82**, 035402 (2010).
[52] M. Abu-samha and L. B. Madsen, Phys. Rev. A **81**, 033416 (2010).
[53] M. Abu-samha and L. B. Madsen, Phys. Rev. A **80**, 023401 (2009).
[54] S. Petretti, Y. V. Vanne, A. Saenz, A. Castro, and P. Decleva, Phys. Rev. Lett. **104**, 223001 (2010).
[55] M. Spanner and S. Patchkovskii, Phys. Rev. A **80**, 063411 (2009).
[56] S.-K. Son and S.-I. Chu, Phys. Rev. A **80**, 011403 (2009).
[57] C. Wu, H. Zhang, H. Yang, Q. Gong, D. Song, and H. Su, Phys. Rev. A **83**, 033410 (2011).
[58] D. Dimitrovski, C. P. J. Martiny, and L. B. Madsen, Phys. Rev. A **82**, 053404 (2010).
[59] V. Kumarappan, L. Holmegaard, C. Martiny, C. B. Madsen, T. K. Kjeldsen, S. S. Viftrup, L. B. Madsen, and H. Stapelfeldt, Phys. Rev. Lett. **100**, 093006 (2008).
[60] The basis sets for CO, CO_2, and OCS are available upon request.